The Plant Cell, Vol. 16, 1327–1339, May 2004, www.plantcell.org © 2004 American Society of Plant Biologists

P-Type ATPase Heavy Metal Transporters with Roles in Essential Zinc Homeostasis in Arabidopsis

Dawar Hussain,[a] Michael J. Haydon,[a] Yuwen Wang,[b] Edwin Wong,[a] Sarah M. Sherson,[a] Jeff Young,[b] James Camakaris,[a] Jeffrey F. Harper,[b] and Christopher S. Cobbett[a,1]

[a] Department of Genetics, University of Melbourne, Australia 3010

[b] Department of Cell Biology, Plant Division, Scripps Research Institute, La Jolla, California, 92037

Arabidopsis thaliana **has eight genes encoding members of the type 1_B heavy metal–transporting subfamily of the P-type ATPases. Three of these transporters, HMA2, HMA3, and HMA4, are closely related to each other and are most similar in sequence to the divalent heavy metal cation transporters of prokaryotes. To determine the function of these transporters in metal homeostasis, we have identified and characterized mutants affected in each. Whereas the individual mutants exhibited no apparent phenotype, *hma2 hma4* double mutants had a nutritional deficiency phenotype that could be compensated for by increasing the level of Zn, but not Cu or Co, in the growth medium. Levels of Zn, but not other essential elements, in the shoot tissues of a *hma2 hma4* double mutant and, to a lesser extent, of a *hma4* single mutant were decreased compared with the wild type. Together, these observations indicate a primary role for HMA2 and HMA4 in essential Zn homeostasis. *HMA2promoter*- and *HMA4promoter*-reporter gene constructs provide evidence that *HMA2* and *HMA4* expression is predominantly in the vascular tissues of roots, stems, and leaves. In addition, expression of the genes in developing anthers was confirmed by RT-PCR and was consistent with a male-sterile phenotype in the double mutant. HMA2 appears to be localized to the plasma membrane, as indicated by protein gel blot analysis of membrane fractions using isoform-specific antibodies and by the visualization of an HMA2-green fluorescent protein fusion by confocal microscopy. These observations are consistent with a role for HMA2 and HMA4 in Zn translocation. *hma2* and *hma4* mutations both conferred increased sensitivity to Cd in a phytochelatin-deficient mutant background, suggesting that they may also influence Cd detoxification.**

INTRODUCTION

Among several families of proteins involved in heavy metal transport across cellular membranes is the type 1_B subfamily of the P-type ATPases. The P-type ATPases transport a variety of cations across cell membranes, and the superfamily can be divided into many subfamilies on the basis of both sequence and functional similarities (Axelsen and Palmgren, 1998). These subfamilies include H^+-ATPases (type 3_A) in plants and fungi, Na^+/K^+-ATPases (type $2_{C/D}$) in animals, Ca^{2+}-ATPases (type $2_{A/B}$), and heavy metal transporting ATPases (type 1_B). Members of the type 4 subfamily have been proposed to transport aminophospholipids.

Type 1_B heavy metal–transporting P-type ATPases have been identified in prokaryotes and eukaryotes, including yeasts, insects, plants, and mammals. In prokaryotes, the metal substrates of these transporters include Cu, Zn, Cd, Ag, Pb, and Co ions, and in most cases, individual transporters confer tolerance to the metal ion substrate through acting as an efflux pump (Rensing et al., 1999). However, some type 1_B ATPases in bacteria appear to play roles in metal uptake and homeostasis (Solioz and Vulpe, 1996; Rutherford et al., 1999). In nonplant eukaryotes, all characterized type 1_B ATPases to date have been identified as Cu transporters. These include CCC2p in yeast and the ATP7A (Menkes) and ATP7B (Wilsons) proteins in humans (Voskoboinik et al., 2002). Biochemical studies using membrane vesicles indicate the substrate for these transporters is Cu(I) rather than Cu(II) (Voskoboinik et al., 2002). Sequence comparisons generally group the type 1_B ATPases into two further classes: those transporting monovalent cations Cu/Ag and those transporting the divalent cations Cd/Pb/Zn/Co (Axelsen and Palmgren, 2001; Cobbett et al., 2003). Eukaryotes for which a complete genome sequence has been published, such as yeast (*Saccharomyces cerevisiae*), Caenorhabditis, Drosophila, and humans, contain only one or two type 1_B ATPases of the Cu/Ag subclass. By contrast, *Arabidopsis thaliana* has eight members of the type 1_B subfamily (Baxter et al., 2003; Cobbett et al., 2003). The nomenclature of these eight members is confused. Baxter et al. (2003) have designated these as HMA1 to HMA8, notwithstanding that two of them, HMA6 and HMA7, have been given previous designations, PAA1 and RAN1, respectively. Here, we will follow the nomenclature of Baxter et al. (2003).

Of the eight members, four of them, HMA5, HMA6 (PAA1), HMA7 (RAN1), and HMA8, are most closely related to the Cu/Ag subclass. HMA7 (RAN1) was first identified in a genetic screen for mutants resistant to an antagonist of the plant hormone ethylene

[1] To whom correspondence should be addressed. E-mail ccobbett@unimelb.edu.au; fax 61-3-83445138.

The authors responsible for distribution of materials integral to the findings presented in this article in accordance with the policy described in the Instructions for Authors (www.plantcell.org) are: Chris Cobbett (ccobbett@unimelb.edu.au) and Jeff Harper (harper@scripps.edu).

Article, publication date, and citation information can be found at www.plantcell.org/cgi/doi/10.1105/tpc.020487.

(Hirayama et al., 1999), and a more severe allele, *ran1-3*, has a constitutive ethylene response phenotype (known as the triple response) (Woeste and Kieber, 2000). Ethylene receptors are Cu-dependent proteins (Hirayama and Alonso, 2000), and loss of function of the receptors presumably through a deficiency in Cu delivery in the *ran1-3* mutant results in a constitutive triple response. In addition, the *ran1-3* mutation causes a seedling lethality, suggesting a failure to deliver Cu to other essential Cu-dependent functions (Woeste and Kieber, 2000). Recent work has demonstrated that HMA6 (PAA1) is responsible for the delivery of Cu to the plastid, particularly the Cu-dependent proteins plastocyanin and Cu/Zn SOD in the plastid. *paa1* mutants have a high chlorophyll fluorescence phenotype arising from impaired photosynthetic electron transport apparently because of a deficiency in holoplastocyanin (Shikanai et al., 2003). The phenotype can be rescued by the addition of excess Cu to the growth medium. HMA5 and HMA8 are most similar in sequence to HMA7 (RAN1) and HMA6 (PAA1), respectively (Baxter et al., 2003). However, their precise functions have not been described.

The remaining four type 1_B ATPases in Arabidopsis, HMA1, HMA2, HMA3, and HMA4, are most closely related to the divalent cation transporters from prokaryotes and have no apparent counterparts in nonplant eukaryotes. The roles of these in heavy metal homeostasis or tolerance in planta have not been described. HMA2, HMA3, and HMA4 are closely related to each other in sequence, and their genes appear to result from duplications through the evolutionary history of Arabidopsis. *HMA2* and *HMA3* are tandem genes on chromosome 4 and lie in a region duplicated on chromosome 2 that contains *HMA4* (Cobbett et al., 2003). A recent publication demonstrated that heterologous expression of HMA4 in *Escherichia coli* restored Zn tolerance to a Zn-sensitive *zntA* mutant but had no effect on the Cu sensitivity of a *copA* mutant and conferred increased Cd resistance in yeast, confirming that HMA4 is a divalent cation transporter (Mills et al., 2003). To further characterize the roles of these genes in planta, we have identified mutant alleles of *HMA2*, *HMA3*, and *HMA4* and demonstrated that *HMA2* and *HMA4* play essential roles in the homeostasis of Zn in Arabidopsis.

RESULTS

T-DNA Insertion Mutant Alleles of *HMA2*, *HMA3*, and *HMA4*

To investigate the function of the three closely related type 1_B P-type ATPase genes, *HMA2*, *HMA3*, and *HMA4*, we have

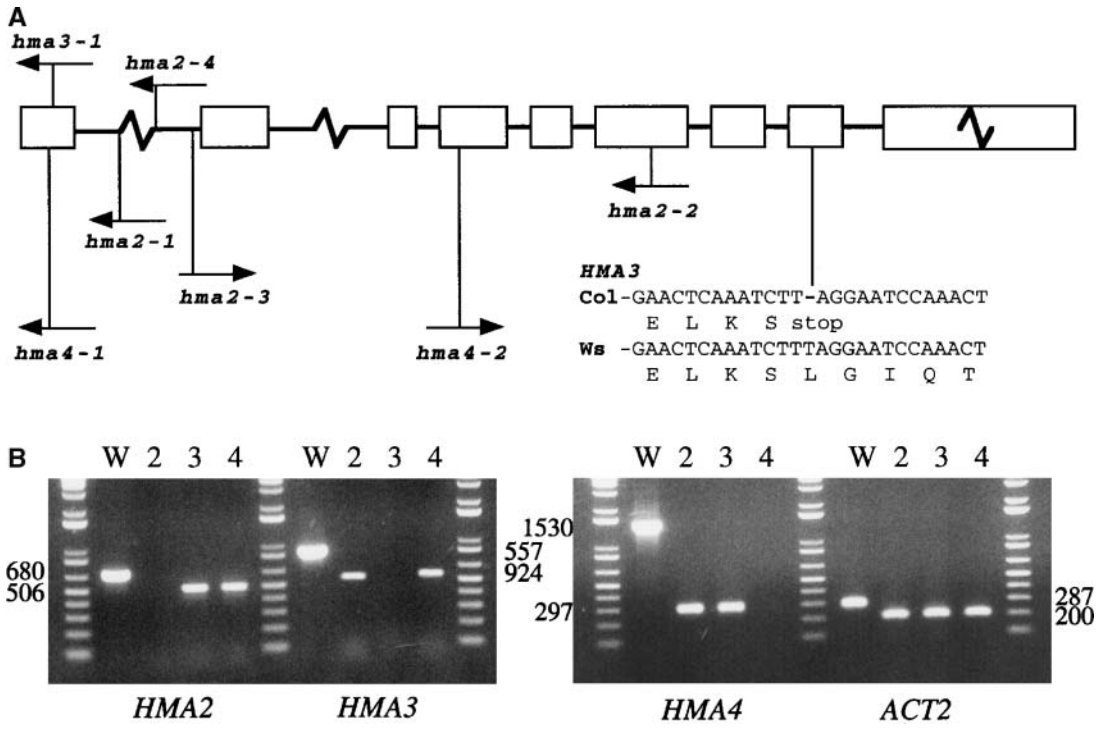

Figure 1. Mutant Alleles of *HMA2*, *HMA3*, and *HMA4*.

(A) A schematic illustration of a composite *HMA* gene. Boxes indicate exon coding sequences and connecting lines indicate introns. Exon and intron sizes are approximately the same for all three genes except that the first two introns and last exon vary considerably in size as indicated by a jagged line. The single base pair deletion polymorphism in *HMA3* between Ws and Col and the relative position of each T-DNA insertion are shown. Arrows indicate T-DNA orientation, with the arrowhead corresponding to the left border. Details of the left border flanking sequences are shown in Table 1.

(B) RT-PCR products obtained using *HMA2*, *HMA3*, *HMA4*, and actin (*ACT2*) gene-specific primers and total RNA isolated from *hma2-2* (2), *hma3-1* (3), and *hma4-1* (4) plants. W indicates a gene-specific fragment amplified from Ws genomic DNA using the same primers. Fragment sizes (bp) are indicated.

identified two independent mutant alleles for each gene. Using a reverse-genetic approach, we identified T-DNA insertion alleles in the Wassilewskija (Ws) ecotype. Five mutant alleles, *hma2-1*, *hma2-2*, *hma2-3*, *hma3-1*, and *hma4-1*, were identified for the three genes. Backcrosses to the wild type, Ws, indicated that the *hma2-2* and *hma3-1* lines contained a single T-DNA locus segregating in a Mendelian ratio. The *hma2-1*, *hma2-3*, and *hma4-1* lines each contained the *hma* mutation and a second independently assorting T-DNA insertion. Lines containing only the *hma* insertion were identified after backcrosses to Ws. We have also obtained *hma* T-DNA insertion lines in the Columbia (Col) ecotype from the SALK collection: SALK_034393, referred to here as *hma2-4*, and SALK_050924, *hma4-2*. In backcrosses to the wild type, these mutants segregated for a single T-DNA.

The positions of the T-DNA left border insertion sites are shown in Figure 1A and Table 1. RT-PCR on total RNA prepared from wild-type and mutant *hma2-2*, *hma3-1*, and *hma4-1* plants was performed using *HMA* gene-specific primers that flanked the T-DNA insertion point. For each mutant, the gene-specific RT-PCR product corresponding to the mutated gene was absent, whereas a product was obtained for the two wild-type *HMA* genes in each mutant (Figure 1B) and for all three genes in the wild type, Ws, control (data not shown).

Comparisons of database sequences of the *HMA3* gene from the Col and Ws ecotypes also indicated that the *HMA3* gene in Col contains a single base pair deletion that would result in a frame shift and subsequent truncation of the predicted gene product after amino acid 542. The truncated product would lack the conserved ATP binding site and is presumably nonfunctional. We have confirmed this polymorphism from both cDNA and genomic DNA in the Col and Ws ecotypes (Figure 1A). For the *hma2 hma4* double mutants in the Ws background described below, we assume that HMA3 is functional, whereas in the Col background, the presence of the naturally occurring *hma3* allele results in a triple mutant line.

hma2 hma4 Double Mutants Show Multiple Phenotypes

When grown in soil, none of the individual *hma* mutants exhibited an apparent phenotype in comparison with the wild type. This may be because of the transporters encoded by these genes having at least partially redundant functions in planta. Much of the Arabidopsis genome has been duplicated through evolution (Blanc et al., 2000), and there are examples where both members of a pair of genes must be mutated to observe a phenotype, thereby indicating overlapping functions. To investigate this possibility, double mutant lines were constructed. The *hma* mutants were crossed, and the F1 progeny were grown and allowed to self-fertilize. The genotypes of F2 individuals were scored by PCR for the absence of the wild-type alleles and then the presence of the gene-specific T-DNA insertions.

In crosses between *hma2* and *hma4* mutants, a small proportion of F2 individuals had a chlorotic stunted phenotype. In a cross segregating for both *hma2-2* and *hma4-1*, 18 individuals with the mutant phenotype were identified in 398 plants ($\chi^2 = 2.3$; $P > 0.05$ for a 1:15 segregation ratio), and all were homozygous for both mutations when genotyped by PCR. Similarly, in a cross between the independent SALK mutant lines *hma2-4* and *hma4-2* in the Col ecotype, 12 of 226 F2 individuals exhibited the same phenotype and were identified as homozygous double mutants ($\chi^2 = 0.03$; $P > 0.8$ for a 1:15 segregation ratio). A total of 76 individuals with a wild-type phenotype were also tested, and all contained a wild-type allele for one or both genes. Together, this demonstrates that the mutant phenotype results from homozygous mutations at both the *hma2* and *hma4* loci.

Because the double mutants failed to grow and set seed, F2 individuals were identified that were homozygous for the *hma4-1* T-DNA insertion but heterozygous for *hma2-2*. Progeny from these were grown in pots and segregated ~25% chlorotic stunted individuals as expected (Figure 2A). These individuals were shown to be homozygous double mutants. By contrast, *hma3-1 hma4-1* double mutant lines were indistinguishable from the wild type. For this reason, the *hma2* and *hma4* single mutants

Table 1. *hma* Mutant Alleles Identified in This Study

Allele[a]	Ecotype	Position[b]	Gene/T-DNA Boundary Sequence (5′/3′)[c]
hma2-1	Ws	Intron 1 (257)	CAAACGTCGTTTTCAG/gatatattca
hma2-2	Ws	Exon 6 (2399)	ACTATCACTAGAGGTGA/tatattcaaa T I T R G
hma2-3	Ws	Intron 1 (580)	cgtcaatgtgtt/AGGTGGGTTTTTACG
hma2-4	Col	Intron 1 (329)	TATTGAGTTACATCT/taataacaca
hma3-1	Ws	Exon 1 (139)	AAAGAATTCTCAGTCA/attgtaaatg K E F S V
hma4-1	Ws	Exon 1 (146)	GGCGTTAAAGAATATT/ctcaggatat G V K E Y
hma4-2	Col	Exon 4 (3439)	tcaatttgtt/AGCTCCACAAAAGGC A P Q K

[a] *hma2-4* is the SALK_034393 insertion line; *hma4-2* is SALK_050924.

[b] Numbers indicate the base pair immediately adjacent to the left border of the T-DNA insertion relative to the A of the predicted initiation codon of the respective gene sequence derived from the Col ecotype.

[c] The slash identifies the boundary between gene sequence and insertion sequence. Gene sequences are in upper case, intron sequences are underlined, coding sequences are translated below, and insertion sequences are in lower case.

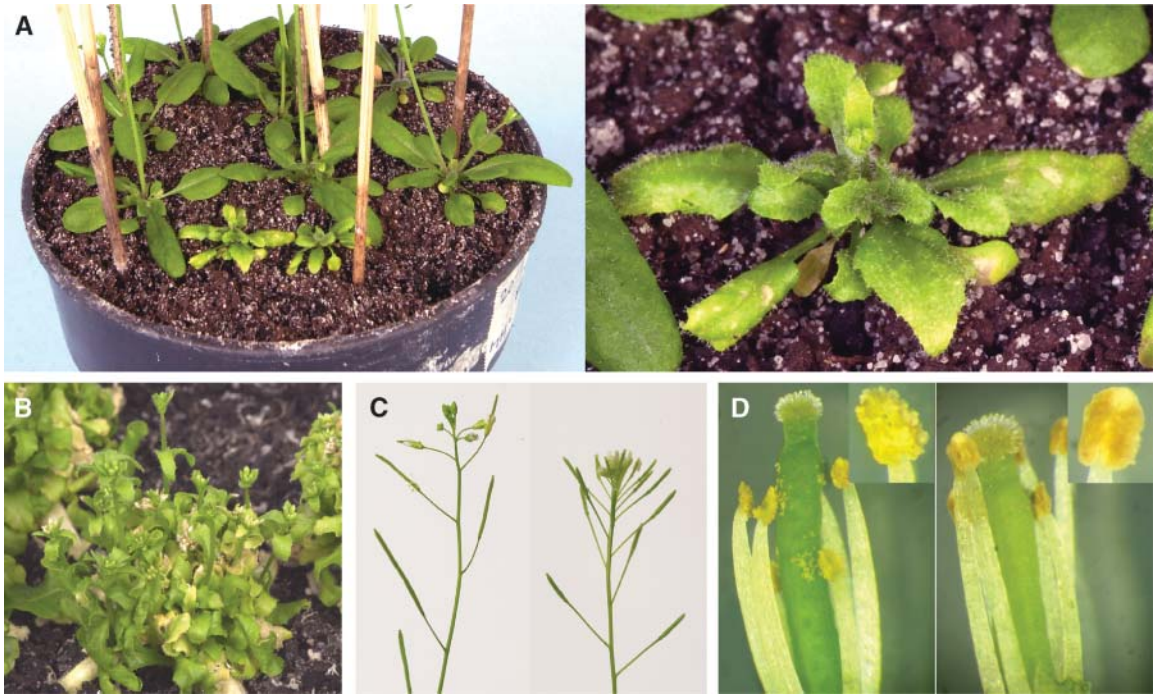

Figure 2. Phenotype of *hma2 hma4* Double Mutant Plants.

(A) Twenty-eight-day-old plants from a population (left) homozygous *hma4-1* and segregating for *hma2-2* with a homozygous *hma2-2 hma4-1* individual shown in detail (right).
(B) Fifty-four-day-old *hma2-2 hma4-1* individual showing multiple aborted bolts.
(C) Inflorescences of wild-type (left) and *hma2-2 hma4-1* mutant (right) plants.
(D) Pistils and anthers of wild-type (left) and *hma2-2 hma4-1* mutant (right) flowers with insets showing dehiscing anthers.

and the *hma2 hma4* double mutant are the focus of the remainder of this study.

The phenotype of the *hma2-2 hma4-1* double mutant is shown in Figure 2. During the early stages of development, the plants were smaller and chlorotic and often appeared to have necrotic patches in the leaves (Figure 2A). Most individuals eventually produced multiple short floral stalks that formed buds but then appeared to abort, resulting in increasingly bushy plants (Figure 2B). In some individuals, the floral stalks extended and developed inflorescences. These inflorescences were more compact than in the wild type because of shortened internodes (Figure 2C). Floral buds and floral organs developed normally, although the anthers produced no pollen (Figure 2D), and the flowers were sterile. The siliques of the double mutant contained no developing embryos and did not elongate and mature as in the wild type (Figure 2C). When mature flowers were cross-pollinated with pollen from a wild-type plant, a few (one to three) embryos formed in each silique but failed to develop into viable seed. This suggests that, in addition to the absence of pollen, there is either a defect in ovule development or, possibly, a failure of fertilized embryos to develop in a homozygous mutant background.

HMA2 and HMA4 Are Involved in Zn Homeostasis

The HMA transporters are most similar to the divalent heavy metal cation subclass of type 1_B P-type ATPases. HMA4 confers increased resistance to Zn or Cd in *E. coli* or yeast (Mills et al., 2003). Thus, we hypothesized that the growth deficiency of the double mutant resulted from Zn deficiency. To investigate this, progeny of a plant homozygous for *hma4-1* and heterozygous for *hma2-2* were planted in pots treated with a single application of standard mineral salts medium (which contains 1 μM Zn). After 21 d, stunted chlorotic individuals could be identified, and those with a wild-type phenotype were removed. The pots were then subirrigated at 3- to 4-d intervals with either water alone or water containing 0.1, 0.3, 1, or 3 mM $ZnSO_4$. Where 0.1 and 0.3 mM Zn solution was applied, growth was increased although variable (data not shown). However, all plants (13) in the pots supplemented with 1 or 3 mM Zn were rescued, with vegetative growth and seed set similar to the wild type (Figure 3A). PCR analysis confirmed that the rescued plants were double homozygous mutants. Identical results were obtained for *hma2-1 hma4-1* double mutants (data not shown). Together, this demonstrates that the growth defect of *hma2 hma4* double mutants results from an extreme Zn deficiency that can be rescued by the application of excess Zn to the soil. Application of Co or Cu to soil was unable to rescue the phenotype (data not shown). The capacity of exogenous Zn application to rescue the growth and fertility of the double mutant allowed it to be maintained as a homozygous double mutant line. Subsequent experiments were performed on seed obtained from homozygous *hma2-2 hma4-1* individuals.

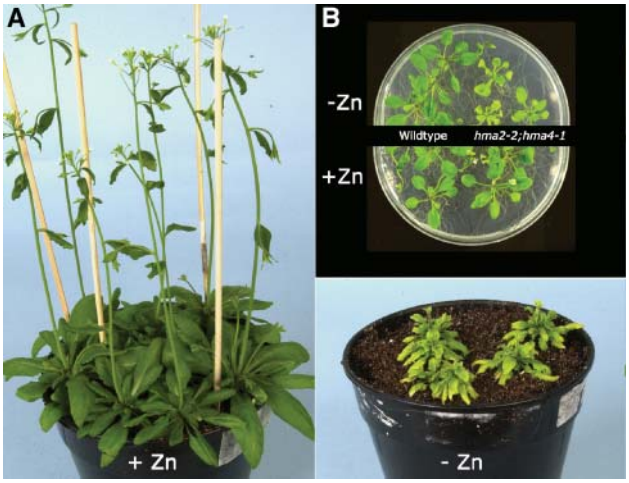

Figure 3. *hma2 hma4* Double Mutant Phenotype Can Be Rescued by Zn.

(A) Twenty-eight-day-old homozygous *hma2-2 hma4-1* plants grown in soil watered with tap water (right, −Zn) or 1 mM $ZnSO_4$ (left, +Zn).
(B) Twenty-one-day-old wild-type and *hma2-2 hma4-1* plants grown on agar mineral salts medium from which Zn was omitted (top, −Zn) or containing 10 μM Zn (bottom, +Zn).

A similar Zn-dependent phenotype was observed for plants grown in agar medium. In this case, the double mutant was indistinguishable from the wild type when grown on mineral salts medium containing 10 μM Zn. However, omitting the Zn from the medium resulted in a similar chlorotic phenotype for the *hma2-2 hma4-1* double mutant but had no effect on the wild type (Figure 3B) or the single mutants (data not shown). The mutant phenotype could not be rescued by the addition of Cu to the medium.

Zn Accumulation in *hma* Mutants

To measure the apparent Zn deficiency, *hma2-2* and *hma4-1* single mutants, the double mutant, and wild-type plants were grown on mineral salts agar medium from which Zn had been omitted or to which 10 μM Zn was added. The levels of Zn accumulated in shoot tissue were measured after 21 d (Figure 4A). In medium to which Zn was not added, the Zn content of the *hma2-2* and *hma4-1* single mutants did not differ significantly from the wild type, whereas in the *hma2-2 hma4-1* double mutant, Zn levels were approximately twofold less than in the wild type and were below the threshold of 20 ppm believed to be required for normal growth (Marschner, 1995). In the presence of 10 μM Zn, the levels of Zn in all lines increased. The *hma2-2* mutant was indistinguishable from the wild type, whereas the *hma4-1* mutant and the double mutant accumulated approximately twofold and fourfold less Zn, respectively, than the wild type. In these same plants, Cu levels (Figure 4B) were not decreased compared with the wild type, and levels of Mg, Mn, Ca, and Fe were not significantly different from the wild type (data not shown), suggesting that the phenotype is attributable to Zn deficiency.

Wild-type and double mutant plants were also grown in soil with and without supplementation with 1 mM Zn. Levels of Zn in

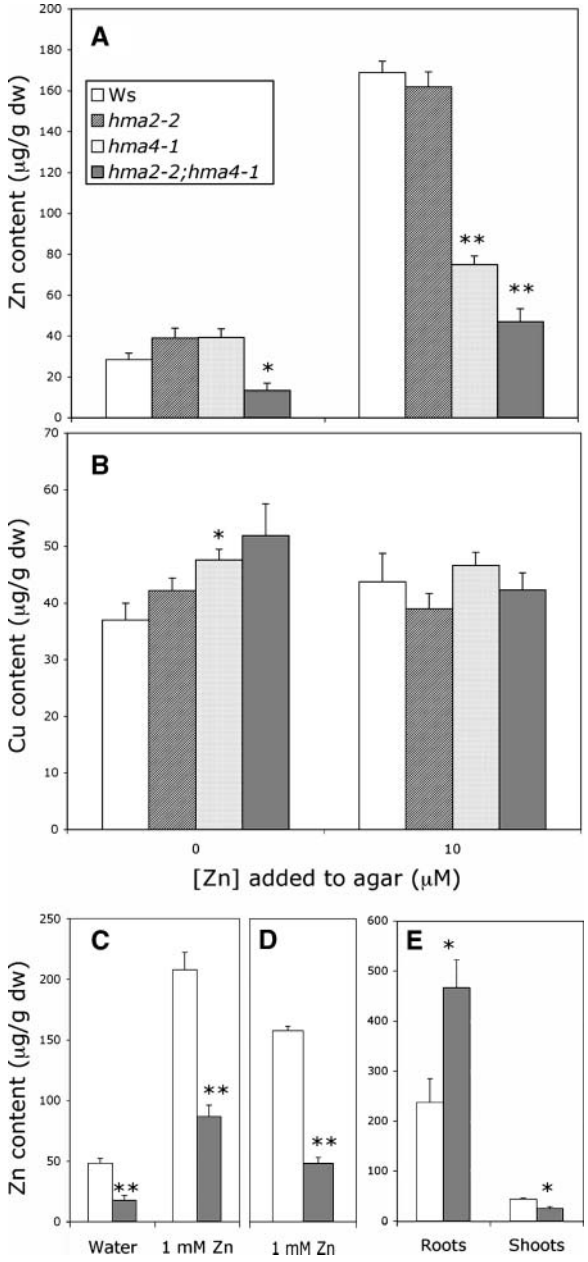

Figure 4. Zn Accumulation in Mutant and Wild-Type Plants.

(A) and **(B)** Zn **(A)** and Cu **(B)** levels in shoots of 21-d-old wild-type, *hma2-2*, *hma4-1*, and *hma2-2 hma4-1* plants grown on agar mineral salts medium from which Zn was omitted (left) or containing 10 μM Zn (right). Values are the mean of 6 ± SE. Significant differences from the wild type as determined by Student's *t* test are indicated by one asterisk ($P < 0.05$) and two asterisks ($P < 0.001$).
(C) Zn levels in rosettes of 26-d-old wild-type and *hma2-2 hma4-1* plants grown in soil irrigated with water or 1 mM $ZnSO_4$.
(D) Zn levels in stems and inflorescences of 32-d-old wild-type and *hma2-2 hma4-1* plants grown in soil irrigated with 1 mM $ZnSO_4$.
(E) Zn levels in roots and shoots of 29-d-old wild-type and *hma2-2 hma4-1* plants grown in hydroponic medium from which Zn had been omitted. Values are the mean ± SE of four samples of tissue pooled from four plants per sample.

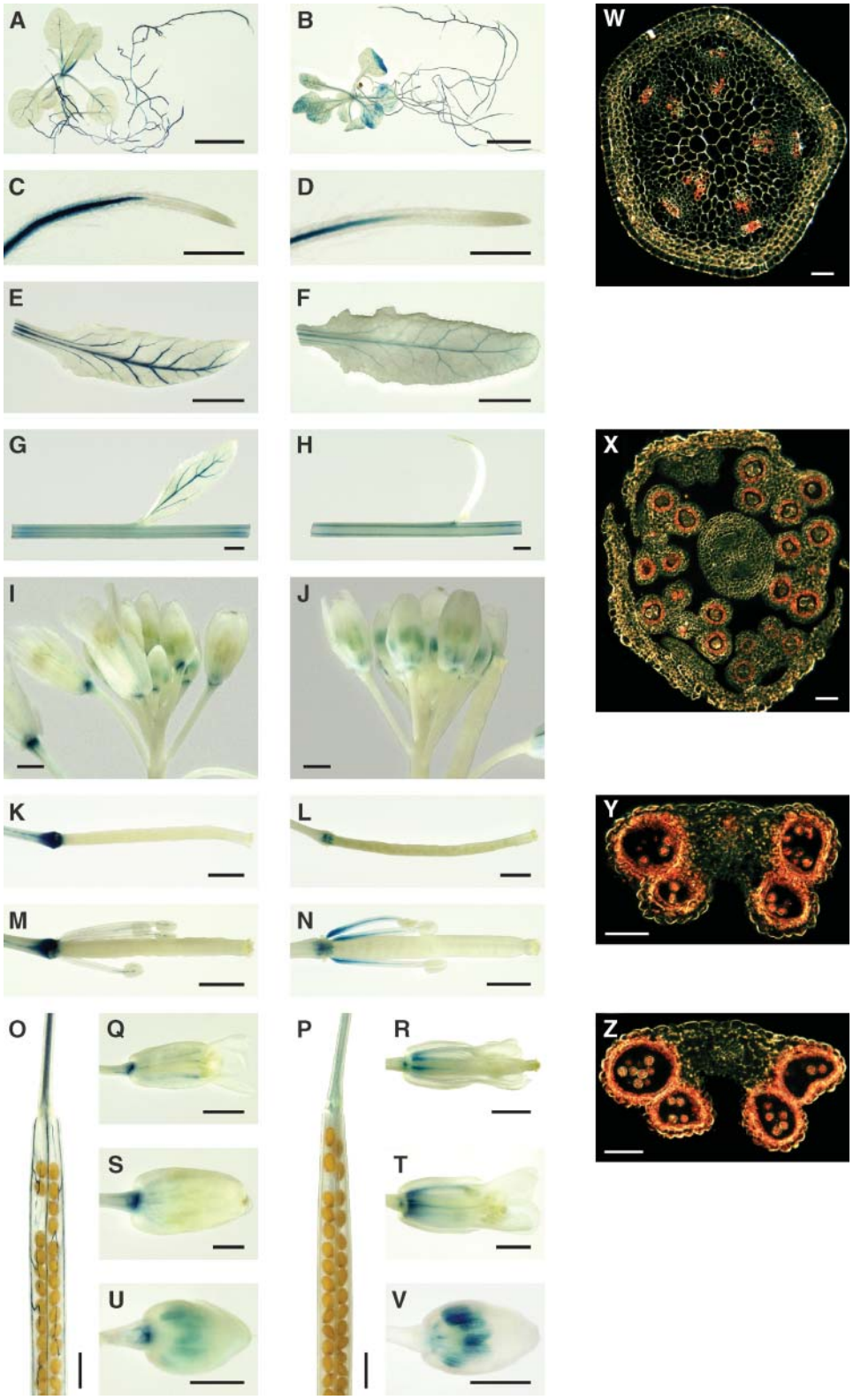

Figure 5. *HMA2p*-GUS and *HMA4p*-GUS Expression in Transgenic Plants.

rosettes of the double mutant were twofold to threefold lower than in the wild type both with and without Zn supplementation (Figure 4C). Plants grown in soil supplemented with 1 mM Zn were allowed to bolt, and stems and inflorescences (but not rosettes) were harvested and measured for Zn content. Under these conditions, growth of the double mutant was indistinguishable from the wild type. Again, in the double mutant, levels of Zn were threefold to fourfold lower than the wild type (Figure 4D). Zn accumulation in roots was also examined in wild-type and double mutant plants grown in hydroponic conditions in medium from which Zn had been omitted (Zn < 0.1 μM). In these plants, the rosettes of the double mutant exhibited the characteristic Zn deficiency phenotype and accumulated approximately twofold less Zn than the wild type as expected (Figure 4E). By contrast, Zn accumulation in roots was approximately twofold higher in the double mutant, indicating that HMA2 and HMA4 are not involved in Zn uptake into roots.

Tissue Specificity of *HMA2* and *HMA4* Expression

To visualize the cellular pattern of *HMA2* and *HMA4* expression in planta, *promoter*-β-glucuronidase (*HMA2p*-GUS and *HMA4p*-GUS) fusion constructs were expressed in transgenic Col plants. For both constructs, GUS expression was predominantly observed in the vascular tissue of roots, leaves, and stems (Figures 5A to 5H). In a section of stem expressing *HMA2p*-GUS, GUS activity was observed in vascular bundles and appeared to be expressed in components of both the xylem and the phloem (Figure 5W). In inflorescences, the expression of both constructs occurred in parallel and changed during floral development (Figures 5I to 5N and 5Q to 5V). In unopened flowers, GUS activity was observed in immature anthers where it was largely confined to the tapetum (Figures 5U and 5V and 5X to 5Z). GUS staining of pollen grains within the anthers was observed in unopened flowers (Figures 5Y and 5Z), although mature pollen did not show GUS activity (data not shown). In opened flowers and senescent flowers, GUS activity was mainly within the vascular tissue of mature anther filaments (Figures 5M, 5N, 5Q, and 5R) and at the base of the developing silique (Figures 5K to 5N). The main qualitative difference in expression of the two constructs was that *HMA2p*-GUS, but not *HMA4p*-GUS, expression was observed in the vascular tissue of mature siliques (Figures 5O and 5P).

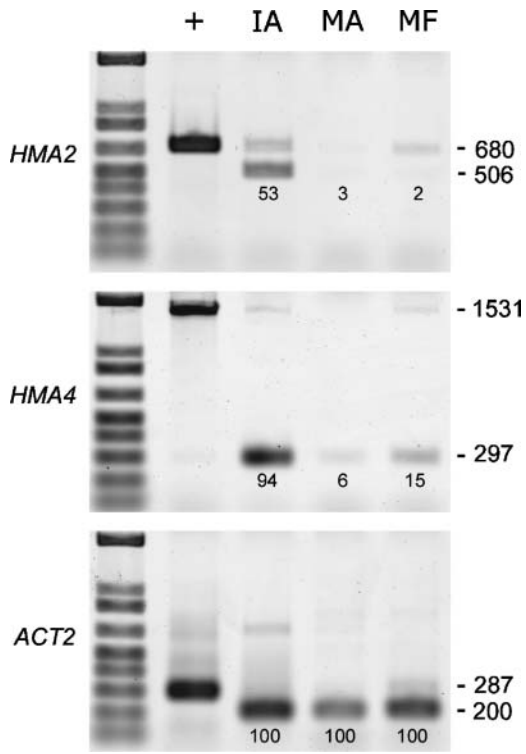

Figure 6. *HMA2* and *HMA4* Expression in Anthers Measured by RT-PCR.

PCR products were amplified using primers specific for *HMA2*, *HMA4*, and actin (*ACT2*) as a control using genomic DNA from Ws plants (+) or cDNA reverse transcribed from RNA isolated from immature (stage 12) anthers (IA), mature anthers (MA), and mature filaments (MF). Intensity of the cDNA band relative to *ACT2* in the same sample is indicated. Fragment sizes for genomic DNA and cDNA products are indicated.

To confirm that the expression of the *promoter*-GUS constructs in anthers reflected the expression of the endogenous genes, we measured *HMA2* and *HMA4* expression directly by RT-PCR. Expression in immature anthers excised from the filaments of unopened stage 12 flowers (Bowman, 1994) was compared with expression in the dehiscing anthers and filaments, separately, of mature opened flowers. Higher levels of both RT-PCR products were detected in immature anthers

Figure 5. (continued).

(A), **(C)**, **(E)**, **(G)**, **(I)**, **(K)**, **(L)**, **(M)**, **(O)**, **(Q)**, **(S)**, **(U)**, **(W)**, **(X)**, and **(Y)** *HMA2p*-GUS transgenic plants.
(B), **(D)**, **(F)**, **(H)**, **(J)**, **(L)**, **(N)**, **(P)**, **(R)**, **(T)**, **(V)**, and **(Z)** *HMA4p*-GUS transgenic plants.
GUS activity is indicated by blue (**[A]** to **[V]**) or red (**[W]** to **[Z]**).
(A) to **(D)** Fourteen-day-old seedling (**[A]** and **[B]**) (bars = 5 mm) with detail of roots (**[C]** and **[D]**) (bars = 0.5 mm).
(E) to **(N)** and **(Q)** to **(V)** Leaf (**[E]** and **[F]**) (bars = 5 mm), stem (**[G]** and **[H]**) (bars = 1 mm), and inflorescence (**[I]** and **[J]**) (bars = 0.5 mm) with developing siliques (**[K]** to **[N]**) and flowers (**[Q]** to **[V]**) of decreasing age from 5-week-old plants. Bars = 1 mm in **(K)** to **(R)** and 0.5 mm in **(S)** to **(V)**.
(O) and **(P)** Mature silique of 7-week-old plant. Bars = 1 mm.
(W) Section of stem of 4-week-old plant. Bar = 10 μm.
(X) Section of unopened flower. Bar = 10 μm.
(Y) and **(Z)** Section through anther of unopened flower. Bars = 10 μm.

compared with mature anthers (Figure 6). Quantitation relative to the actin control revealed a 10- to 20-fold difference in expression (Figure 6). Expression of both *HMA2* and *HMA4* in mature filaments was also detected by RT-PCR. The pattern of expression in anthers observed using RT-PCR reflected that in the *promoter*-GUS transgenic plants.

HMA2 Is Localized to the Plasma Membrane

Two different approaches were used to identify the subcellular location of HMA2. First, total membranes from plants were fractionated by aqueous two-phase partitioning, and the fractions were characterized by protein gel blot analysis probed with HMA2-specific antibodies. The specificity of the antibodies was confirmed by probing protein gel blots of microsomal proteins extracted from wild-type and *hma2-3* mutant plants (Figure 7A). Aqueous two-phase partitioning preferentially partitions plasma membrane into the upper phase, and the other membranes, including endoplasmic reticulum (ER), Golgi, chloroplast membrane, and tonoplast, into the lower phase (Schaller and DeWitt, 1995). Figure 7B shows that HMA2 is enriched in the upper phase, as was a plasma membrane H^+-ATPase marker, AHA2 (Dewitt et al., 1996). Controls indicated that endomembranes were enriched in the lower phase, as shown using antibodies that recognized an ER membrane–located Ca^{2+}-ATPase, ACA2 (Hong et al., 1999), and the tonoplast-located γTIP (Johnson et al., 1990).

To corroborate the plasma membrane localization, HMA2 was fused in frame with a green fluorescent protein (GFP) and expressed under the control of the 35S promoter of *Cauliflower mosaic virus* in transgenic plants. The HMA2-GFP fusion protein was confirmed to be enriched in upper-phase plasma membrane fractions by protein gel blots probed with GFP-specific antibody and HMA2-specific antibody (Figure 7B). The subcellular location of the HMA2-GFP protein in root tip cells was visualized by confocal microscopy (Figures 8A and 8B). The pattern of fluorescence is consistent with the plasma membrane location indicated by membrane fractionation. In a control expressing GFP protein alone, fluorescence was observed within the nucleus and throughout the cytoplasm (Figure 8C), consistent with a previous report (Haseloff et al., 1997).

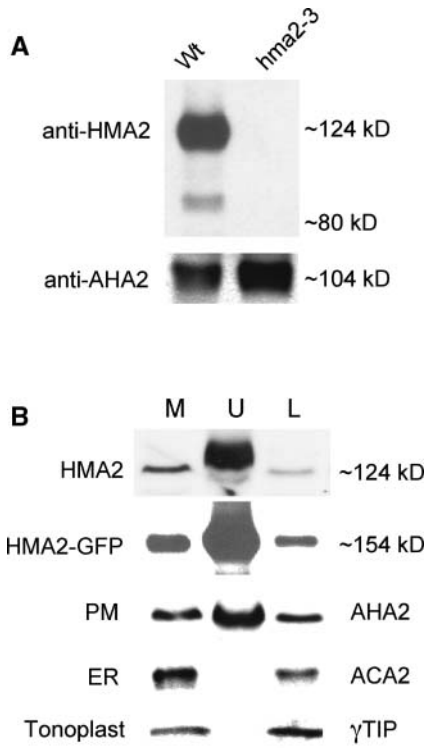

Figure 7. Membrane Localization of HMA2 by Protein Gel Blot Analysis.

(A) Protein gel blot analysis of microsomal fractions from wild type (Wt) Ws, and mutant *hma2-3* plants. Equal amounts of protein (10 μg) were loaded in each lane. Sizes and positions of standards are indicated.

(B) Protein gel blot analysis of plant membrane fractions from two-phase partitioning fractionation probed with antibodies that recognize HMA2, HMA2-GFP, a plasma membrane (PM)-located H^+-ATPase, AHA2, an ER-located Ca^{2+}-ATPase, ACA2, and tonoplast-located γTIP. M, total membrane proteins; U, plasma membrane–enriched upper phase proteins; L, endomembrane-enriched lower phase proteins. Equal amounts of protein were loaded in each lane. All membrane fractions were from wild-type Ws plants, except for samples probed with the anti-GFP antibody, which were from a plant line overexpressing an HMA2-GFP fusion (Figure 8). Equivalent results were obtained in two independent experiments. Approximate sizes are indicated.

hma2 and *hma4* Mutations Increase Sensitivity to Cd in a Phytochelatin-Deficient Background

The single *hma* mutants were tested for altered sensitivity to Zn, Cd, and Co in agar medium, and no distinct phenotype was observed (data not shown). Because HMA4 is able to confer increased Cd resistance when expressed in yeast (Mills et al., 2003), we wished to investigate a possible role for HMA2 and HMA4 in Cd resistance. In Arabidopsis, the major determinant of Cd detoxification is the phytochelatins (PCs), and *cad1-3*, PC synthase-deficient mutants lacking detectable PCs show an approximately 40-fold increase in Cd sensitivity (Howden et al., 1995; Ha et al., 1999). Thus, it was possible that a slight effect on Cd sensitivity mediated by the *hma* mutations may have been masked by the presence of PCs. To test this, *hma2-1* and *hma4-1* mutants were crossed with the *cad1-3* mutant. Among F2 populations, individuals that exhibited the extreme Cd sensitivity of *cad1-3* homozygotes were observed at a frequency of ~25% (data not shown) and were subsequently screened by PCR to identify those homozygous for the *hma* T-DNA insertion. Progeny from these *hma cad1-3* double mutant lines were then tested for sensitivity to Cd. The *hma2-1 cad1-3* and *hma4-1 cad1-3* mutants exhibited approximately twofold increased sensitivity to Cd compared with the *cad1-3* mutant alone. In the presence of 0.15 μM Cd, growth of all three strains was inhibited to some extent, but inhibition of the *hma cad1-3* lines was significantly greater than for the *cad1-3* mutant alone (Figure 9). In the presence of 0.06 μM Cd, only the *hma4-1 cad1-3* line was inhibited compared with *cad1-3*, and in the presence of 0.3 μM Cd, all three lines were equally inhibited.

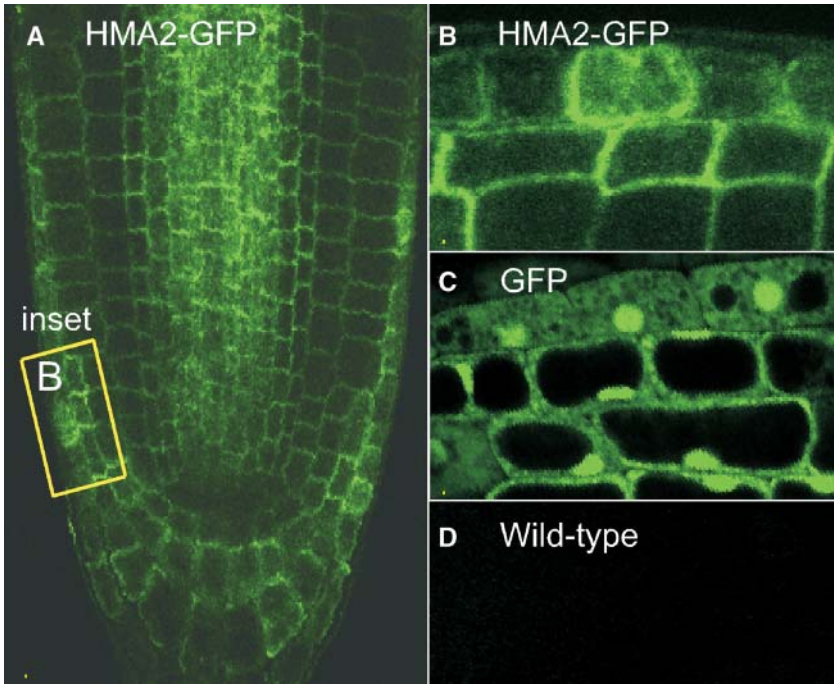

Figure 8. Membrane Localization of HMA2-GFP Fusion.

(A) Confocal fluorescence image of a root tip expressing an HMA2-GFP fusion protein.
(B) Detail of box shown in **(A)**.
(C) Confocal fluorescence image of a root tip expressing a GFP control.
(D) Confocal fluorescence image of a root tip of a wild-type control under the same exposure settings used in **(A)**.

DISCUSSION

On the basis of amino acid sequence comparisons, the HMA2, HMA3, and HMA4 transporters in Arabidopsis are grouped with the divalent heavy metal–transporting subgroup of P-type ATPases (Baxter et al., 2003; Cobbett et al., 2003; Mills et al., 2003). The data described here provide evidence that HMA2 and HMA4 play an important role in Zn transport and homeostasis in planta. The *hma4* mutant and *hma2 hma4* double mutant have decreased Zn accumulation, and the latter has a deficiency phenotype that can be compensated for by the application of additional exogenous Zn. The double mutant phenotype is characteristic of previously reported Zn deficiency symptoms observed in other species. These symptoms include uneven chlorosis in leaves of reduced size, rosetting of leaves on a stem because of shortened internodes—a phenotype particularly apparent in the inflorescence of the double mutant—and infertility (Marschner, 1995).

The *hma2 hma4* double mutant phenotype can be suppressed solely by the addition of Zn to the agar or soil medium, indicating that the primary role of these transporters is likely to be in the uptake or translocation of Zn. Whether these transporters have a secondary role in the transport of any other essential metals has not been explored directly. With respect to Cu, no differences in Cu levels in the mutants compared with the wild type were observed, and the omission or addition of Cu in agar medium or soil had no effect on the deficiency phenotype of the *hma2 hma4* double mutant. In addition, previous work has shown that HMA4 is unable to rescue the Cu sensitivity of a *copA* mutant of *E. coli* (Mills et al., 2003). Possible roles of the HMA transporters in Cd resistance are discussed below.

The observation that only the *hma2 hma4* double mutant and neither of the single mutants exhibited an obvious nutritional deficiency in soil suggests that HMA2 and HMA4 have a level of functional redundancy. This is consistent with earlier sequence comparisons that show that HMA4 is more closely related to HMA2 than to HMA3 and with the largely parallel patterns of expression of the *HMA2p*-GUS and *HMA4p*-GUS reporter constructs. Nonetheless, at the level of the cell or the tissue, the two transporters may serve different functions in Zn transport. The observation that the double mutant accumulates more, rather than less, Zn in roots indicates that these transporters are not involved in Zn uptake from soil and is consistent with an inability to translocate Zn from root tissue. The reduced level of Zn accumulated in both rosette and stem tissues of the *hma2 hma4* double mutant that was observed under conditions of both visible Zn deficiency and Zn supplementation also indicates that these transporters are involved in the translocation of Zn to various tissues of the plant. The expression of the *promoter*-GUS reporter constructs in the vascular tissue of roots, leaves, and stems is consistent with a role in the translocation of Zn. HMA2 and HMA4 may play a role in the loading or unloading of Zn in the

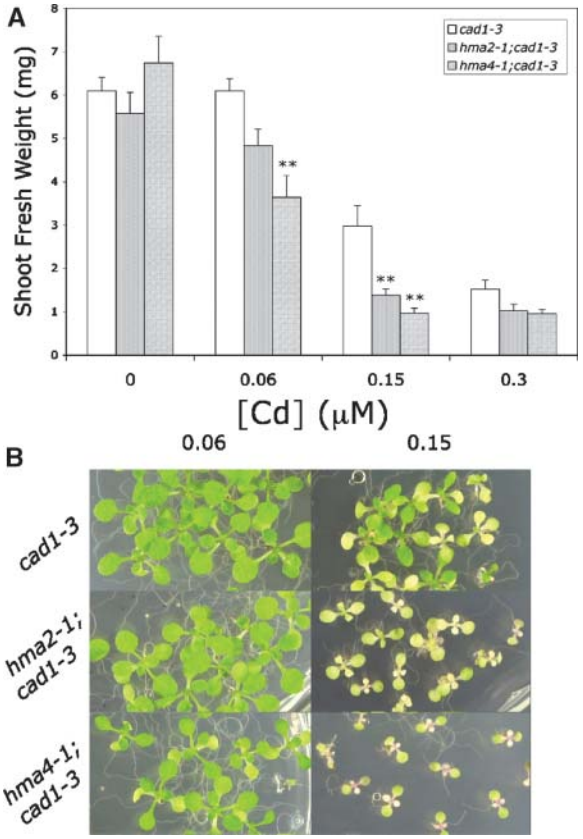

Figure 9. Cd Sensitivity of *hma cad1-3* PC-Deficient Mutants.

(A) Plants were grown in the presence or absence of added Cd and shoot fresh weight determined after 14 d. Values are the mean of 10 plants ± SE. Significant differences from the wild type as determined by Student's *t* test are indicated by two asterisks ($P < 0.01$).
(B) Plants growing in the presence of 0.06 or 0.15 μM Cd.

xylem. Expression of both is also observed in phloem tissue and may indicate a role in the remobilization of Zn from shoot to root. The subcellular localization of HMA2 to the plasma membrane is consistent with transporting Zn into or out of cells and supports a role for HMA2 in the translocation of Zn within the plant.

A striking feature of the double mutant phenotype is sterility, particularly the absence of fertile pollen. This may arise from a systemic Zn deficiency or may be more directly attributable to the loss of function of these transporters in specific reproductive tissues. Fertility appears to be most sensitive to Zn depletion in the double mutant. When Zn is no longer applied to fully fertile plants rescued by Zn supplementation, infertility is the first visible effect (data not shown). This is consistent with the measurement of high Zn concentrations in pollen of bean (*Phaseolus vulgaris*) and tobacco (*Nicotiana tabacum*), much of which was incorporated into embryos at fertilization (Polar, 1975). The *HMA2p*-GUS and *HMA4p*-GUS constructs are both expressed in developing anthers, particularly the tapetum, and RT-PCR experiments have confirmed expression of both *HMA2* and *HMA4* mRNA in this tissue. Thus, it seems likely that these transporters play a specific role in the delivery of Zn to male reproductive tissues. Their role in female reproductive tissues has not been determined.

The *hma3-1* mutation either alone or in combination with *hma4-1* produced no apparent phenotype. However, these lines have not been extensively analyzed for Zn or Cd uptake and accumulation. Thus, even in the absence of a visible phenotype, *hma3* mutations may influence Zn and/or Cd localization. The wild-type Col ecotype appears to be an *hma3* mutant because the *HMA3* gene contains a single base pair deletion that would result in a frame shift and subsequent truncation of the gene product. The mutants described here in detail have been isolated in the Ws background in which we presume HMA3 is functional. Thus, an *hma2 hma3* double mutant has not been isolated by recombination because these are tandem genes and the appropriate recombinant would be a rare event. However, the *hma2-4* and *hma4-2* insertion mutants in the Col ecotype are presumably *hma2 hma3* and *hma3 hma4* double mutants, respectively. Neither of these has an apparent phenotype, and the *hma2-3 hma4-2* double mutant, which is presumably a triple mutant, was phenotypically similar to the *hma2-2 hma4-1* double mutant in the Ws background. Nonetheless, more detailed analysis of Zn levels in these different mutant combinations may identify a specific role for HMA3. In the Zn hyperaccumulator *Arabidopsis halleri*, the *HMA3* ortholog is more highly expressed (>100-fold) than in Arabidopsis (Col ecotype) and has been proposed to play an important role in Zn hyperaccumulation (Becher et al., 2004). However, because the allele of *HMA3* in Arabidopsis (Col ecotype) has a premature termination codon, its transcript may be subject to nonsense-mediated decay, and the observed difference in expression may be unrelated to Zn accumulation.

Although the level of Zn in the shoot tissues of the *hma2-2 hma4-1* double mutant was always less than in the wild type, supplementation of either agar or soil growth medium with additional Zn increased the level of Zn in the double mutant and rescued the phenotype to the wild type. This indicates that, notwithstanding the loss of function of HMA2 and HMA4, sufficient Zn can be translocated throughout the plant provided that enough is supplied to the roots. The mechanism by which this is achieved is unclear but may rely upon other Zn transporters. Other transporters may include members of the ZIP or CDF families of transporters that are also known to transport Zn in plants (Guerinot, 2000; Maser et al., 2001). Under sufficiently high Zn concentrations, phenotypic rescue may also involve nonspecific transport by other mechanisms. There has also been speculation that some Zn transport in plants may be via the apoplasm (Ernst et al., 2002; White et al., 2002). In any case, it will be of interest to determine the specific roles of the various types of Zn transporters in Arabidopsis in the uptake and distribution of Zn throughout plant tissues.

In prokaryotes, many of the divalent cation P-type ATPases transport both Zn and Cd. The analysis of the *hma cad1-3* double mutants indicates both HMA2 and HMA4 influence Cd resistance in vivo. HMA4 when expressed in yeast confers increased resistance to Cd (Mills et al., 2003), although direct measurement of Cd transport by HMA4 has not been reported. Nonetheless, it is possible that HMA2 and HMA4 are able to transport Cd, and the *hma* mutations influence Cd accumulation in specific tissues,

thereby increasing Cd sensitivity in a PC-deficient background. Alternatively, it may be that increased sensitivity to Cd is an indirect effect of perturbations in Zn homeostasis. Because the crosses to generate these combinations were between parents of the Col and Ws ecotypes, they also involved the *hma3* point mutation in the Col allele in addition to the *cad1-3* (Col) allele and the *hma2* or *hma4* (Ws) alleles. However, the *HMA3* genotype has not been determined in the lines used for testing Cd sensitivity. Because *HMA3* is adjacent to *HMA2*, it is reasonable to expect that the *cad1-3 hma2-1* double mutant carries the apparently wild-type Ws *HMA3* allele. However, in the *cad1-3 hma4-1* double mutant, the *HMA3* alleles may be derived from either the Col or Ws parent. Thus, it is possible the Cd-sensitive phenotype in the *cad1-3 hma4-1* line tested is contributed to by the Col *hma3* mutant allele.

In summary, we suggest that the primary function of HMA2 and HMA4 is in Zn translocation. These can be added to the increasing number of transporters involved in Zn transport in plants. Orthologous transporters may play important roles in the delivery of Zn to edible portions of crop plants and, thus, in their nutritional value. They may also be important in the mobilization of Zn to the aerial tissues of Zn hyperaccumulator species such as *A. halleri* (Baker and Whiting, 2002) and *Thlaspi caerulescens* (Assuncao et al., 2003). It seems that a role in Cd resistance by these transporters is not of great physiological significance in Arabidopsis. Other mechanisms of Cd detoxification, such as the PCs, play a more significant role. Notwithstanding this, in hyperaccumulator species, HMA orthologs may play a more significant role in Cd accumulation.

METHODS

Plant Materials and Genotype Determination

Arabidopsis thaliana plants were grown in agar and soil as described previously (Howden et al., 1995). Plants were grown hydroponically according to Tocquin et al. (2003), except that the nutrient solution consisted of one-quarter strength medium without Zn. The *hma* mutants in the Ws ecotype were identified in PCR screens of a collection of T-DNA–inserted kanamycin-resistant Arabidopsis lines (Krysan et al., 1999) using primers specific for sequences flanking the coding sequences of each of the *HMA* genes and a T-DNA left border–specific primer. All except *hma2-3* were identified with the assistance of the Wisconsin Arabidopsis knockout service. Information about the *hma* mutants in the Col ecotype was obtained from the SIGnAL Web site at http://signal.salk.edu, and seed was obtained from ABRC (Alonso et al., 2003). The T-DNA insertion point was determined by nucleotide sequence analysis of the left border PCR fragment. The genotype of plants was determined by PCR using primers flanking the insertion point for the wild-type allele and a gene-specific and left border–specific primer pair for the insertion allele. For RT-PCR analysis of gene expression in the mutants, total RNA was isolated from 15-d-old plants. cDNA was synthesized using the Superscript first-strand synthesis system (Invitrogen, Carlsbad, CA) and amplified using gene-specific primers that flanked the positions of the T-DNA inserts.

Inductively Coupled Plasma Atomic Emission Spectroscopy Determination of Metal Content

Plant tissue was harvested, dried at 60°C for 3 d, and weighed and digested in 70% HNO_3 overnight at room temperature and then at 80°C for 2 h. Hydroponically grown plants were rinsed in water, washed in 5 mM MES-Tris, pH 6.0, 5 mM $CaCl_2$, and 10 mM EDTA for 15 min, blotted dry, and separated into roots and shoots before drying. Metal content was measured using inductively coupled plasma AES with a Vista-AX (Varian, Melbourne, Australia) instrument.

Promoter-GUS Fusion Construct Lines

The regions upstream of *HMA4* and *HMA2* from −5920 to +97 were amplified by PCR and digested at internal restriction sites. Fragments of *HMA4* from −4765 to +164 (relative to the A of the predicted start codon) and of *HMA2* from −5920 to +97 were cloned and subsequently ligated into pBI101 (Clontech, Palo Alto, CA) in fusion with the GUS-NOSt cassette. The *promoter*-GUS constructs were transformed into Col plants via the *Agrobacterium tumefaciens*-mediated floral dip method (Clough and Bent, 1998). At least 14 independent homozygous transgenic lines for each construct were tested for GUS activity, and of these, >80% showed a consistent staining pattern. Two lines of each construct were selected for further analysis. The histochemical localization of GUS activity was performed according to the method adapted from Jefferson et al. (1987). Sections (8 μm) were prepared for dark-field microscopy according to Johnson et al. (2002), except that staining was for 16 h. Under the conditions used, the blue product of the GUS reaction appears red.

Quantitative RT-PCR of Anther mRNA

Six anthers from a single unopened (stage 12; Bowman, 1994) flower and anthers and filaments from a mature flower from a single wild-type Col plant were collected. Tissue was ground immediately using acid-washed sand, and RNA was extracted using an RNeasy plant mini kit (Qiagen, Valencia, CA). cDNA was synthesized using a Sensiscript reverse transcriptase kit (Qiagen). PCR was performed with gene-specific primers using 10 μL of the cDNA product in a 50-μL reaction with 30 reaction cycles. In each case, primers were designed to span at least one intron to distinguish cDNA amplification products from genomic DNA contaminants. Two microliters of each reaction were electrophoresed on a 3-mm 1% agarose gel and stained with SYBR Green 1 (Sigma, St. Louis, MO) according to the manufacturer's instructions. Fluorescence was visualized using a Typhoon 9410 variable mode imager (Amersham Pharmacia Biotech, Uppsala, Sweden). Image analysis and quantitation was performed using ImageQuant Version 5.2 (Amersham Pharmacia Biotech).

Expression of an HMA2-GFP Fusion Construct in Transgenic Plants

The full-length open reading frame encoding HMA2 was fused to GFP in the vector p35S-GFP-JFH1 (Hong et al., 1999) and expressed downstream from the 35S promoter of *Cauliflower mosaic virus* and a tobacco etch virus translational enhancer (Harper et al., 1998). Transgenic plants were generated by a vacuum-infiltration method using *A. tumefaciens* strain GV3101 (Bechtold et al., 1993) and selected using 50 μM Basta (DL-Phosphinothricin; Sigma). For fluorescence confocal microscopy, plant root tips were excised from 4-week-old plants grown on Gamborg's B5 agar medium and treated with Slowfade-antifade reagent in PBS buffer (Molecular Probes, Eugene, OR). Images were collected by using a confocal laser-scanning microscope (Olympus Fluoview; Olympus, Tokyo, Japan) attached to an inverted microscope (Olympus 1X70) equipped with a fluorescein filter. The thickness of the optical section was 0.5 μm.

Isolation of an HMA2-Specific Antibody and Protein Gel Blot Analysis of Membrane Fractions

A DNA fragment encoding the C-terminal 251 amino acid residues of HMA2 (HMA2-C) was fused to glutathione *S*-transferase in the expression

vector pGEX-KG (Guan and Dixon, 1991) and to the maltose binding protein in expression vector pMAL-CR1 (New England Biolabs, Beverly, MA). Both fusion proteins were expressed in *Escherichia coli* and purified using corresponding affinity columns. The glutathione *S*-transferase-HMA2-C fusion protein was used to immunize rabbits, and a polyclonal antiserum was obtained. Maltose binding protein-HMA2-C was cross-linked to a cyanogen bromide activated Sepharose 4B matrix (Pharmacia Biotech, Piscataway, NJ) according to the manufacturer's instructions and was used to affinity purify anti-HMA2-C–specific antibodies from the antiserum. The specificity of the antibodies was confirmed by probing protein gel blots of microsomal proteins extracted from wild-type and *hma2-3* mutant plants. No proteins were bound by the antibody in protein gel blots of extracts from the *hma2-3* mutant (Figure 7A).

Microsomal membranes were purified and fractionated by aqueous two-phase partitioning using the method of Schaller and DeWitt (1995). For protein gel blot analysis, proteins were electrophoresed by SDS-PAGE, transferred to nitrocellulose membranes, blocked for at least 6 h in TBS-T (Tris-buffered saline and 0.2% [v/v] Tween 20) buffer with 5% nonfat dry milk, and incubated for 2 to 4 h with primary antisera diluted in TBS-T buffer with 2% dry milk (anti-HMA2-C at 1:250; anti-ACA2 at 1:2000 [Hong et al., 1999]; anti-AHA2 at 1:5000 [DeWitt et al., 1996]; anti-γTIP at 1:500 [provided by M. Chrispeels]; and GFP antibody at 1:50 (Clonetech, San Fransisco, CA). The secondary antibody was a donkey anti-rabbit IgG conjugated with horseradish peroxidase (Amersham, Buckinghamshire, UK) used at 1:4000 dilution in TBS-T with 2% nonfat dry milk and was detected by enhanced chemiluminescence (Amersham) or Supersignal-West Dura extended duration substrate (Pierce, Rockford, IL).

The Arabidopsis Information Resource locus identifiers are as follows: *HMA2*, At4g30110; *HMA3*, At4g30120; *HMA4*, At2g19110. Sequence data (for cDNA sequences) from this article have been deposited in the EMBL/GenBank data libraries under the following accession numbers: AV554840, *AtHMA4* cDNA Col ecotype; AY434728, *AtHMA2* cDNA Col ecotype; AY434729, *AtHMA3* cDNA Ws ecotype; AY434730, *AtHMA3* cDNA Col ecotype. The accession numbers for insertion mutants are as follows: *hma2-4*, SALK_034393; *hma4-2*, SALK_050924.

ACKNOWLEDGMENTS

The authors wish to acknowledge the Wisconsin Arabidopsis knockout service, the Salk Institute Genomic Analysis Laboratory for providing the sequence-indexed Arabidopsis T-DNA insertion mutants, Maarten Chrispeels for the anti-γTIP antisera, Steven Whiting, Augustine Doronila, Scott Laidlaw, and Alan Baker for assistance with and access to the inductively coupled plasma AES, and John Golz and David Smyth for assistance with tissue sectioning and analysis. Quentin Lang has provided excellent assistance with photography and graphics. This work was supported by grants to C.S.C. by the Australian Research Council and to J.F.H. by the Department of Energy (Grant DE-FG03-94ER20152) and the National Science Foundation (Grant DBI-0077378).

Received December 23, 2003; accepted February 26, 2004.

REFERENCES

Alonso, J.M., et al. (2003). Genome-wide insertional mutagenesis of *Arabidopsis thaliana*. Science **301,** 653–657.

Assuncao, A.G.L., Schat, H., and Aarts, M.G.M. (2003). *Thlaspi caerulescens*, an attractive model species to study heavy metal hyperaccumulation in plants. New Phytol. **159,** 351–360.

Axelsen, K.B., and Palmgren, M.G. (1998). Evolution of substrate specificities in the P-type ATPase superfamily. J. Mol. Evol. **46,** 8–101.

Axelsen, K.B., and Palmgren, M.G. (2001). Inventory of the superfamily of P-type ion pumps in Arabidopsis. Plant Physiol. **126,** 696–706.

Baker, A.J.M., and Whiting, S.N. (2002). In search of the Holy Grail—A further step in understanding metal hyperaccumulation? New Phytol. **155,** 1–4.

Baxter, I., Tchieu, J., Sussman, M.R., Boutry, M., Palmgren, M.G., Gribskov, M., Harper, J.F., and Axelsen, K.B. (2003). Genomic comparison of P-Type ATPase ion pumps in Arabidopsis and rice. Plant Physiol. **132,** 618–628.

Becher, M., Talke, I.N., Krall, L., and Kramer, U. (2004). Cross-species microarray transcript profiling reveals high constitutive expression of metal homeostasis genes in shoots of the zinc hyperaccumulator *Arabidopsis halleri*. Plant J. **37,** 251–268.

Bechtold, N., Ellis, J., and Pelletier, G. (1993). In planta *Agrobacterium*-mediated gene transfer by infiltration of adult *Arabidopsis thaliana* plants. C. R. Acad. Sci. Life Sci. **316,** 1194–1199.

Blanc, G., Barakat, A., Guyot, R., Cooke, R., and Delseny, I. (2000). Extensive duplication and reshuffling in the Arabidopsis genome. Plant Cell **12,** 1093–1101.

Bowman, J. (1994). Arabidopsis: An Atlas of Morphology and Development. (New York: Springer-Verlag).

Clough, S.J., and Bent, A.F. (1998). Floral dip: A simplified method for Agrobacterium-mediated transformation of *Arabidopsis thaliana*. Plant J. **16,** 735–743.

Cobbett, C.S., Hussain, D., and Haydon, M.J. (2003). Structural and functional relationships between type 1_B heavy metal-transporting P-type ATPases in Arabidopsis. New Phytol. **159,** 315–321.

DeWitt, N.D., Hong, B., Sussman, M., and Harper, J.F. (1996). Targeting of two *Arabidopsis* H^+-ATPase isoforms to the plasma membrane. Plant Physiol. **112,** 833–844.

Ernst, W.H.O., Assuncao, A.G.L., Verkleij, J.A.C., and Schat, H. (2002). How important is apoplastic zinc xylem loading in *Thlaspi caerulescens*? New Phytol. **155,** 4–5.

Guan, K.L., and Dixon, J.E. (1991). Eukaryotic proteins expressed in *Escherichia coli*: An improved thrombin cleavage and purification procedure of fusion proteins with glutathione S-transferase. Anal. Biochem. **192,** 262–267.

Guerinot, M.L. (2000). The ZIP family of metal transporters. Biochim. Biophys. Acta **1465,** 190–198.

Ha, S.-B., Smith, A.P., Howden, R., Dietrich, W.M., Bugg, S., O'Connell, M.J., Goldsbrough, P.B., and Cobbett, C.S. (1999). Phytochelatin synthase genes from *Arabidopsis* and the yeast *Schizosaccharomyces pombe*. Plant Cell **11,** 1153–1164.

Harper, J.F., Hong, B., Hwang, I., Guo, H.Q., Stoddard, R., Huang, J.F., Palmgren, M.G., and Sze, H. (1998). A novel calmodulin-regulated Ca^{2+}-ATPase (ACA2) from *Arabidopsis* with an N-terminal autoinhibitory domain. J. Biol. Chem. **273,** 1099–1106.

Haseloff, J., Siemering, K.R., Prasher, D.C., and Hodge, S. (1997). Removal of a cryptic intron and subcellular localization of green fluorescent protein are required to mark transgenic *Arabidopsis* plants brightly. Proc. Natl. Acad. Sci. USA **94,** 2122–2127.

Hirayama, T., and Alonso, J.M. (2000). Ethylene captures a metal! Metal ions are involved in ethylene perception and signal transduction. Plant Cell Physiol. **41,** 548–555.

Hirayama, T., Kieber, J.J., Hirayama, N., Kogan, M., Guzman, P., Nourizadeh, S., Alonso, J.M., Dailey, W.P., Dancis, A., and Ecker, J.R. (1999). Responsive-to-antagonist1, a Menkes/Wilson disease-related copper transporter, is required for ethylene signaling in Arabidopsis. Cell **97,** 383–393.

Hong, B., Ichida, A., Wang, Y., Gens, J.S., Pickard, B.G., and Harper, J.F. (1999). Identification of a calmodulin-regulated Ca^{2+}-ATPase in the endoplasmic reticulum. Plant Physiol. **119,** 1165–1176.

Howden, R., Goldsbrough, P.B., Andersen, C.R., and Cobbett, C.S. (1995). Cadmium-sensitive, *cad1*, mutants of *Arabidopsis thaliana* are phytochelatin deficient. Plant Physiol. **107,** 1059–1066.

Jefferson, R.A., Kavanagh, T.A., and Bevan, M.W. (1987). GUS fusions: Beta-glucuronidase as a sensitive and versatile gene fusion marker in higher plants. EMBO J. **20,** 3901–3907.

Johnson, C.S., Kolevski, B., and Smyth, D.R. (2002). *TRANSPARENT TESTA GLABRA2*, a trichome and seed coat development gene of Arabidopsis, encodes a WRKY transcription factor. Plant Cell **14,** 1359–1375.

Johnson, K.D., Hofte, H., and Chrispeels, M.J. (1990). An intrinsic tonoplast protein of protein storage vacuoles in seeds is structurally related to a bacterial solute transporter (GIpF). Plant Cell **2,** 525–532.

Krysan, P.J., Young, J.C., and Sussman, M.R. (1999). T-DNA as an insertional mutagen in Arabidopsis. Plant Cell **11,** 2283–2290.

Marschner, H. (1995). Mineral Nutrition of Higher Plants. (London: Academic Press).

Maser, P., et al. (2001). Phylogenetic relationships within cation transporter families of Arabidopsis. Plant Physiol. **126,** 1646–1667.

Mills, R.F., Krijger, G.C., Baccarini, P.J., Hall, J.L., and Williams, L.E. (2003). Functional expression of AtHMA4, a P-1B-type ATPase of the Zn/Co/Cd/Pb subclass. Plant J. **35,** 164–176.

Polar, E. (1975). Zinc in pollen and its incorporation into seeds. Planta **123,** 97–103.

Rensing, C., Ghosh, M., and Rosen, B.P. (1999). Families of soft-metal-ion-transporting ATPases. J. Bacteriol. **181,** 5891–5897.

Rutherford, J.C., Cavet, J.S., and Robinson, N.J. (1999). Cobalt-dependent transcriptional switching by a dual-effector MerR-like protein regulates a cobalt-exporting variant CPx-type ATPase. J. Biol. Chem. **274,** 25827–25832.

Schaller, G.E., and DeWitt, N.D. (1995). Analysis of the H(+)-ATPase and other proteins of the *Arabidopsis* plasma membrane. Methods Cell Biol. **50,** 129–148.

Shikanai, T., Müller-Moulé, P., Munekage, Y., Niyogi, K.K., and Pilon, M. (2003). PAA1, a P-Type ATPase of Arabidopsis, functions in copper transport in chloroplasts. Plant Cell **15,** 1333–1346.

Solioz, M., and Vulpe, C. (1996). CPx-type ATPases: A class of P-type ATPases that pump heavy metals. Trends Biochem. Sci. **21,** 237–241.

Tocquin, P., Corbesier, L., Havelange, A., Pieltain, A., Kurtem, E., Bernier, G., and Périlleux, C. (2003). A novel high efficiency, low maintenance, hydroponic system for synchronous growth and flowering of *Arabidopsis thaliana*. BMC Plant Biol. **3,** 2.

Voskoboinik, I., Camakaris, J., and Mercer, J.F.B. (2002). Understanding the mechanism and function of copper P-type ATPases. Adv. Protein Chem. **60,** 123–150.

White, P.J., Whiting, S.N., Baker, A.J.M., and Broadley, M.R. (2002). Does zinc move apoplastically to the xylem in roots of *Thlaspi caerulescens*? New Phytol. **153,** 201–207.

Woeste, K.E., and Kieber, J.J. (2000). A strong loss-of-function mutation in *RAN1* results in constitutive activation of the ethylene response pathway as well as a rosette-lethal phenotype. Plant Cell **12,** 443–455.

P-Type ATPase Heavy Metal Transporters with Roles in Essential Zinc Homeostasis in Arabidopsis

Dawar Hussain, Michael J. Haydon, Yuwen Wang, Edwin Wong, Sarah M. Sherson, Jeff Young, James Camakaris, Jeffrey F. Harper and Christopher S. Cobbett

PLANT CELL 2004;16;1327-1339; originally published online Apr 20, 2004;
DOI: 10.1105/tpc.020487